Applicability of molecular simulations for modelling the adsorption of the greenhouse gas CF_4 on carbons

Applicability of molecular simulations for modelling the adsorption of the greenhouse gas CF₄ on carbons

**Sylwester Furmaniak[1], Artur P Terzyk[1], Piotr A Gauden[1],
Piotr Kowalczyk[2], Peter J F Harris[3] and Stanisław Koter[4]**

[1] Department of Chemistry, Physicochemistry of Carbon Materials Research Group, N Copernicus
University, Gagarin Street 7, 87-100 Toruń, Poland
[2] Nanochemistry Research Institute, Department of Chemistry, Curtin University of Technology,
PO Box U1987, Perth, 6845 Western Australia, Australia
[3] Centre for Advanced Microscopy, University of Reading, Whiteknights, Reading RG6 6AF, UK
[4] Department of Chemistry, Chair of Physical Chemistry and Physicochemistry of Polymers,
N Copernicus University, Gagarin Street 7, 87-100 Toruń, Poland

E-mail: sf@chem.umk.pl and p.j.f.harris@reading.ac.uk

Abstract
Tetrafluoromethane, CF_4, is a powerful greenhouse gas, and the possibility of storing it in
microporous carbon has been widely studied. In this paper we show, for the first time, that the
results of molecular simulations can be very helpful in the study of CF_4 adsorption. Moreover,
experimental data fit to the results collected from simulations. We explain the meaning of the
empirical parameters of the supercritical Dubinin–Astakhov model proposed by Ozawa and
finally the meaning of the parameter k of the empirical relation proposed by Amankwah and
Schwarz.

S Online supplementary data available from stacks.iop.org/JPhysCM/25/015004/mmedia

(Some figures may appear in colour only in the online journal)

1. Introduction

Perfluorocarbons, due to their high stability and low
chemical reactivity have found application in microelectronics
for cleaning or printing electronic circuit boards, in
semiconductor industry, and also during the process of
aluminum production [1, 2]. The simplest perfluorocarbon,
tetrafluoromethane (CF_4), is known as a particularly powerful
greenhouse gas. It absorbs IR radiation more effectively than
CO_2. Considering the lifetime of this gas in the atmosphere
(50 000 years) leads to the conclusion that during a 100 year
period CF_4 is 6500 times more harmful than CO_2 [1, 2].
Taking this into account there have been many attempts to
find a simple and effective method of CF_4 storage. Some
methods used for this purpose are based on the application of
adsorption phenomena, and among adsorbents a crucial role
has been played by activated carbons [1, 2].

It is well known that activated carbons are widely used
for the adsorption of pollutants from gaseous as well as
from liquid phases [3–7]. Experimental studies reporting CF_4
adsorption data on carbons usually present only isotherms,
and/or sometimes a comparison is presented with adsorption
of other adsorbates [8–11]. There are however, exceptions. For
example Jagiełło *et al* [9] considered the possibility of using
CF_4 for determining the pore size distribution of activated
carbons. However, generally, there is a lack of literature data
reporting systematic experimental studies on CF_4 adsorption
on carbons with gradually changed porosity.

The major purpose of this study is to assess the
applicability of molecular simulations for prediction of carbon
adsorption properties towards the powerful greenhouse gas
CF_4. Its storage was studied recently using the Monte Carlo
simulation technique [1, 2], however, the results published
in the literature were limited only to slit-like micropores

and to ideal carbon nanotubes. Therefore, there are no theoretical studies in the literature on CF_4 storage on realistic carbon models. This is regrettable, given that realistic models take into account pore connectivity, heterogeneity, disordered carbon structure etc, i.e. fundamental properties of real carbons.

Among realistic carbon structures the Virtual Porous Carbon (VPC) models are the most important [12–15]. Among the major advantages of VPC application we mention well defined porosity and defined chemical composition of carbon surface layer. Thus, contrary to experiment, we know everything about our VPC sample. Additionally, by a simple geometric manipulation we can easily change the porosity of VPC in a systematic way [15].

Another important consideration is that since in real carbons there is an interrelation between the porosity and the chemical composition of the carbon surface layer, it is very hard to obtain a series of samples with progressively changed porosity. On the other hand, this is very simple for the case of VPC models. This is why in the present study we collected experimental data of CF_4 adsorption on commercially available carbons and additionally, we performed theoretical description of them. Next, using a series of VPC based on models proposed by Harris *et al* [16–22] and Monte Carlo simulations we explore the general relationships between theoretical parameters of the widely used Dubinin–Astakhov (DA) adsorption model [23–26] and carbon CF_4 storage properties. Experimental data fit quite well to simulation results. Our relations can be very useful for predicting effective CF_4 adsorbents. Moreover, we show for the first time for CF_4, that the empirical parameter k of the supercritical version of the DA model is strictly related to the pore diameter of the activated carbon sample.

2. Methodology

2.1. Experimental data of CF_4 adsorption on commercial carbons

The data for CF_4 adsorption on commercial carbons are tabulated in the literature. We used the data published by Ahn *et al* ($T = 303$, 323 and 343 K; this carbon is labelled in our study as AC) [11] and three sets of data published by Jagiełło *et al* [8] for carbon molecular sieve Carbosieve G ($T = 258$, 275 and 296 K) and activated carbons Westvaco ($T = 268$, 283 and 297 K) and Maxsorb ($T = 268$, 283 and 296 K). The sets of adsorption isotherms were described by the supercritical version of the DA adsorption isotherm equation [26]:

$$a(p, T) = a_0(T) \times \exp\left[-\left(\frac{A(p, T)}{E}\right)^n\right] \quad (1)$$

where a_0 is the maximum adsorption (limited by the volume of pores), E is the characteristic energy of adsorption (formally the product of the characteristic energy and the affinity coefficient), n is the best-fit parameter related to the heterogeneity of an adsorbent, and A is the adsorption

potential defined as:

$$A(p, T) = RT \times \ln \frac{p_s^*}{p} \quad (2)$$

where R is the universal gas constant and p_s^* is the apparent saturated vapour pressure for supercritical conditions, calculated by the relation proposed by Amankwah and Schwarz [27]:

$$p_s^* = p_C \times \left(\frac{T}{T_C}\right)^k \quad (3)$$

where $p_C = 3.75$ MPa and $T_C = 227.51$ K are the critical parameters of CF_4, and k is the value characterizing an adsorption system. The temperature dependence of maximum adsorption was estimated using the relation proposed by Ozawa *et al* [28]:

$$a_0(T) = a_0^B \times \exp[-\alpha(T - T_B)] \quad (4)$$

where a_0^B is the value of maximum adsorption at the boiling point $T_B = 145.10$ K, and $\alpha = 0.0025$ $1/K$ is the thermal expansion coefficient of an adsorbate.

In order to describe the datasets by the DA model (equations (1)–(4)), we used the genetic algorithm proposed by Storn and Price [29], applied by us recently for the description of different datasets (see for example [25, 26, 30–33]). We used exactly the same procedure as described in [26]. The best-fit parameters were a_0^B, E, n and k. The fit for each isotherm was checked using the value of determination coefficient:

$$DC_T = 1 - \eta_T \quad (5)$$

where:

$$\eta_T = \frac{\sum_i (a_{exp,i} - a_{theo,i})^2}{\sum_i (a_{exp,i} - a_{exp,av})^2} \quad (6)$$

$a_{exp,i}$ and $a_{theo,i}$ denote the experimental (or simulated—see below) and theoretical adsorption values for the ith adsorption point, respectively, and $a_{exp,av}$ is the average experimental (or simulated) adsorption value. The global fitting parameter for a branch of isotherms is defined as:

$$DC = 1 - \sqrt{\frac{\sum_T \eta_T^2}{3}} \quad (7)$$

where 3 in the denominator denotes the number of temperature values. The procedure of standard deviation of the best-fit parameters calculation is described in supplementary data (available at stacks.iop.org/JPhysCM/25/015004/mmedia).

2.2. Molecular simulation

We used a series of VPC described in [34] (selected examples are shown in figure 1). The starting structure was S0 (see figure 1) composed of fullerene-like fragments (the model proposed by Harris *et al*). Additional structures were created by a random incorporation of small carbon fragments. In this way we obtained a series of 10 VPC models with
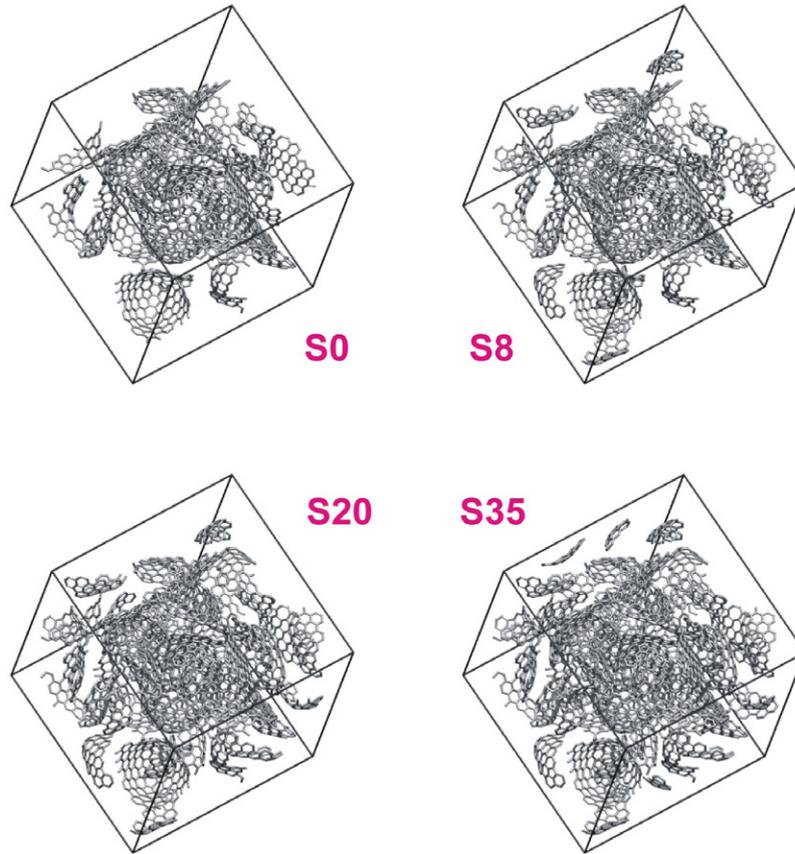
Figure 1. The structure of selected VPC samples (frames reflect the size of the simulation box).

systematically changed porosity (we labelled the structures as: S0, S4, S8, S12, S16, S20, S24, S28, S32, S35). All VPC models were placed in cubic simulation boxes (4.6 nm × 4.6 nm × 4.6 nm) with periodic boundary conditions in all three dimensions.

The porosity of VPCs was described using the procedure proposed by Bhattacharya and Gubbins (BG) [35]. During the calculation, for each structure a uniform grid (100×100×100) of points was generated in the box. For each point (located in a pore), the largest sphere containing this point and situated in the pore was found in an iterative way (for details see for example [36, 37]). Its diameter corresponds with the size of the pore containing the point. The collection of the data for all the points makes it possible to determine the histogram of pore sizes (i.e. the probabilities of finding the pores having the given effective diameter (d_{eff})–$P(d_{eff})$). The integral curves connected with the histograms were also calculated [37]:

$$P_{int}(d_{eff}) = \sum_{d \leq d_{eff}} P(d). \tag{8}$$

The $P_{int}(d_{eff})$ value provides the information on what percentage of pores has a diameter not larger than d_{eff}. The obtained histograms were also used to calculate the average pore diameter of pores accessible for CF$_4$ molecules ($d_{eff,acc,av}$):

$$d_{eff,acc,av} = \frac{\sum_{d_{eff} \geq 0.47 \text{ nm}} d_{eff} \times P(d_{eff})}{\sum_{d_{eff} \geq 0.47 \text{ nm}} P(d_{eff})}. \tag{9}$$

The lower diameter of pores assumed by us (0.47 nm) reflects the collision diameter of a CF$_4$ molecule (see below).

Adsorption isotherms were simulated using the method proposed by Yan and de Pablo and known as hyper parallel tempering Monte Carlo (HPTMC) [38]. For each VPC we used 123 replicas for temperature 283, 298 and 313 K, respectively, and the values of pressure from ca. 1 Pa up to ca. 6 MPa. The HPTMC simulations utilized 1×10^7 cycles (one cycle = 100 attempts of the change of each replica state by (i) creation, (ii) annihilation or (iii) displacement of a randomly chosen molecule with equal probabilities, and one attempt at a configuration swap between a pair of randomly chosen replicas). The first 2×10^6 cycles were discarded to guarantee equilibration.

Each CF$_4$ molecule and each carbon atom building the VPCs were modelled as a simple Lennard-Jones (LJ) centre [39]. The potential energy of interactions was calculated using the truncated LJ potential [39]. The following values of collision diameters (σ) and potential well depth (ε) were used for CF$_4$: $\sigma_{ff} = 0.47$ nm, $\varepsilon_{ff}/k_B = 152.27$ K (k_B—is the Boltzmann constant) [1], and for C atoms: $\sigma_{ss} = 0.34$ nm, $\varepsilon_{ss}/k_B = 28$ K [40]. The Lorentz–Berthelot rule was used for the calculation of parameters for mixed interactions [39]. For each type of interactions, the cut-off distance was assumed as equal to $4.5 \times \sigma_{ij}$.

The average number of Ar atoms in each replica ($\langle N \rangle$) corresponds to the adsorption amount. We calculated the
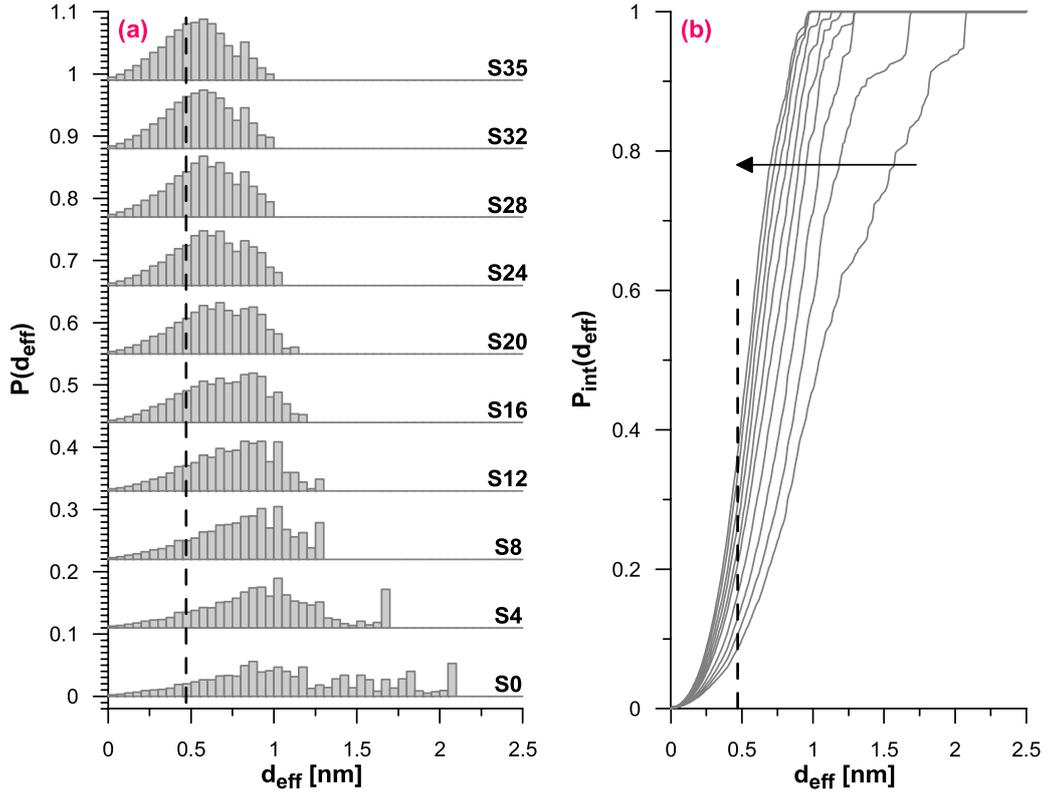
Figure 2. (a) Histograms of pore diameters for virtual porous carbons (dashed line represents the collision diameter of the CF$_4$ molecule). (b) The integral curves related to the histograms (the arrow shows the direction of changes from structure S0 up to S35).

absolute adsorption per unit of carbon mass:

$$a_{abs} = \frac{\langle N \rangle}{N_C \times M_C} \quad (10)$$

where N_C is the number of carbon atoms in a given VPC structure, and M_C is the molar mass of carbon. Adsorption excess (a_{exc}) was calculated from:

$$a_{exc} = \frac{\langle N \rangle - \rho_{bulk} \times V_{acc}}{N_C \times M_C} \quad (11)$$

where ρ_{bulk} is the density of gaseous CF$_4$ for given p and T, and V_{acc} is the volume of pores accessible for CF$_4$ in a given VPC structure. V_{acc} was computed using Monte Carlo integration. The size of pores (limiting their accessibility) was determined analogously as in the above described BG method. In order to illustrate the degree of filling of pores accessible for the adsorbate, the CF$_4$ density in pores was also calculated:

$$\rho = \frac{\langle N \rangle}{N_{Av} \times V_{acc}} \quad (12)$$

where N_{Av} is the Avogadro's number. The isosteric enthalpy of adsorption (q^{st}) was calculated from the theory of fluctuations.

Simulated adsorption isotherms were described using the DA model (equations (1)–(4)) and the same procedure was applied as used for the description of experimental data.

3. Results and discussion

Figure 2 shows histograms of pore diameters for the studied VPC structures, and the integral pore size distribution curves. All structures are microporous, and one can observe systematic changes in porosity from the structure S0 up to S35. The changes are caused by progressive filling of larger pores by carbon fragments during an MC creation of new structures [34]. One can also see that with the progressive filling of structure S0 by carbon fragments the volume of pores accessible for CF$_4$ molecules decreases (see dashed line in figure 2).

Figure 3 shows the results of the GCMC simulation (for $T = 298$ K; however, for the remaining temperatures similar regularities are observed). One can observe a systematic decrease in absolute and excess adsorption values with the decrease in average pore diameter. This is the result of the internal VPC structure, i.e. the decrease in pore volume and the rise in the mass of carbon with the rise in microporosity. The observed decrease in a_{exc} for larger pressures is caused by a smaller rise in the adsorbed amount than the increase in density of gaseous CF$_4$.

If one considers the changes in density of adsorbed molecules (figures 3(c) and (d)) the opposite effect is observed i.e. the density increases in the opposite direction to adsorption, and this is caused by the increasing potential energy with the decrease in pore diameters. This is especially
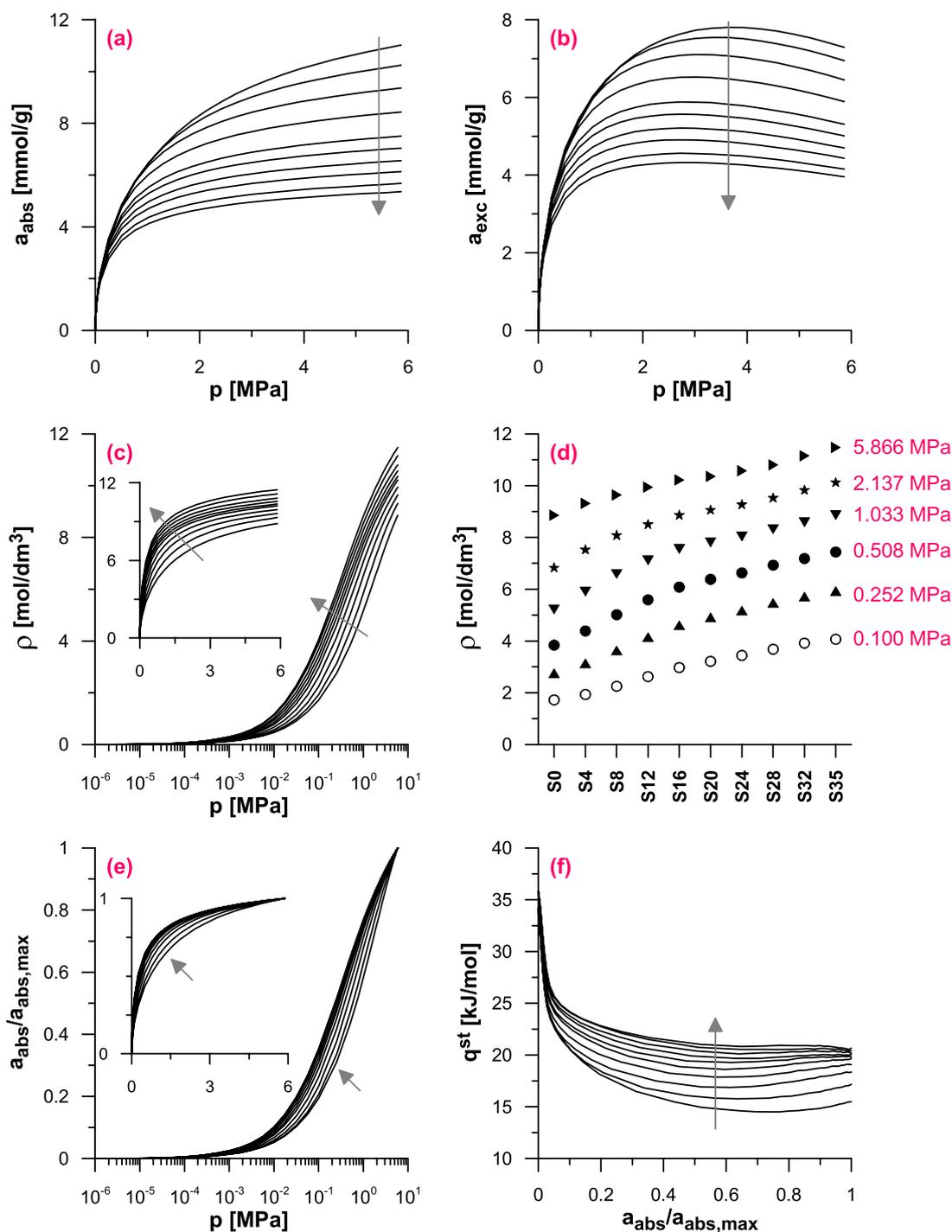
Figure 3. Comparison of simulation results for $T = 298$ K. (a) Absolute adsorption, (b) excess adsorption, (c) CF_4 density in pores, (d) comparison of densities in pores for selected pressures, (e) relative adsorption, (f) isosteric adsorption enthalpy plots. The arrows show the direction of changes from structure S0 up to S35.

seen on the relative adsorption and adsorption enthalpy plots (figures 3(e) and (f)).

The influence of porosity on adsorption isotherms and energetics of the process is smallest at low pressures. At small fillings CF_4 molecules are adsorbed inside curved fragments of the fullerene-like structure. Next, at larger pressures, during adsorption on low energetic sites (and during the filling of the whole pore space) one can observe the effect caused by

the rise in adsorption potential in smaller pores. Therefore, in smaller pores the volume is utilized by molecules more efficiently, and the pressure necessary to reach a given density decreases from S0 down to the S35 VPC structure (figure 3(d)).

The results of fitting experimental and selected simulated datasets by the DA model (equations (1)–(4)) are presented in figure 4 and values obtained for the best-fit parameters are
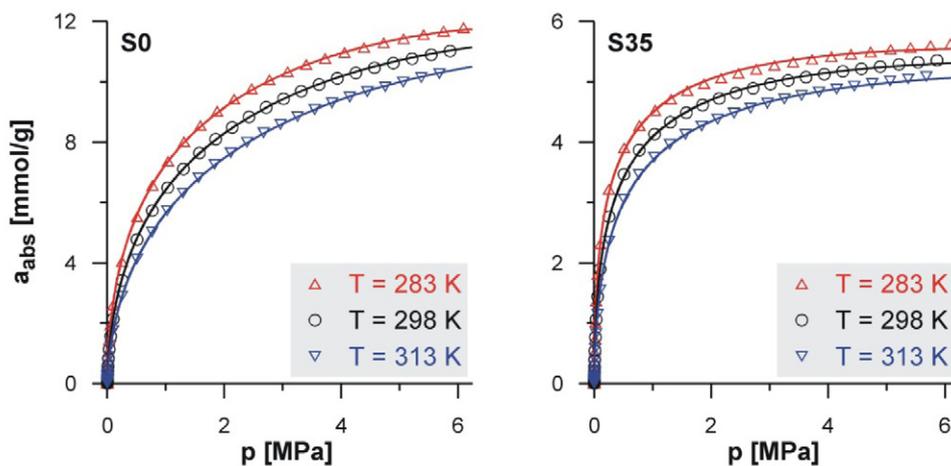
EXPERIMENT
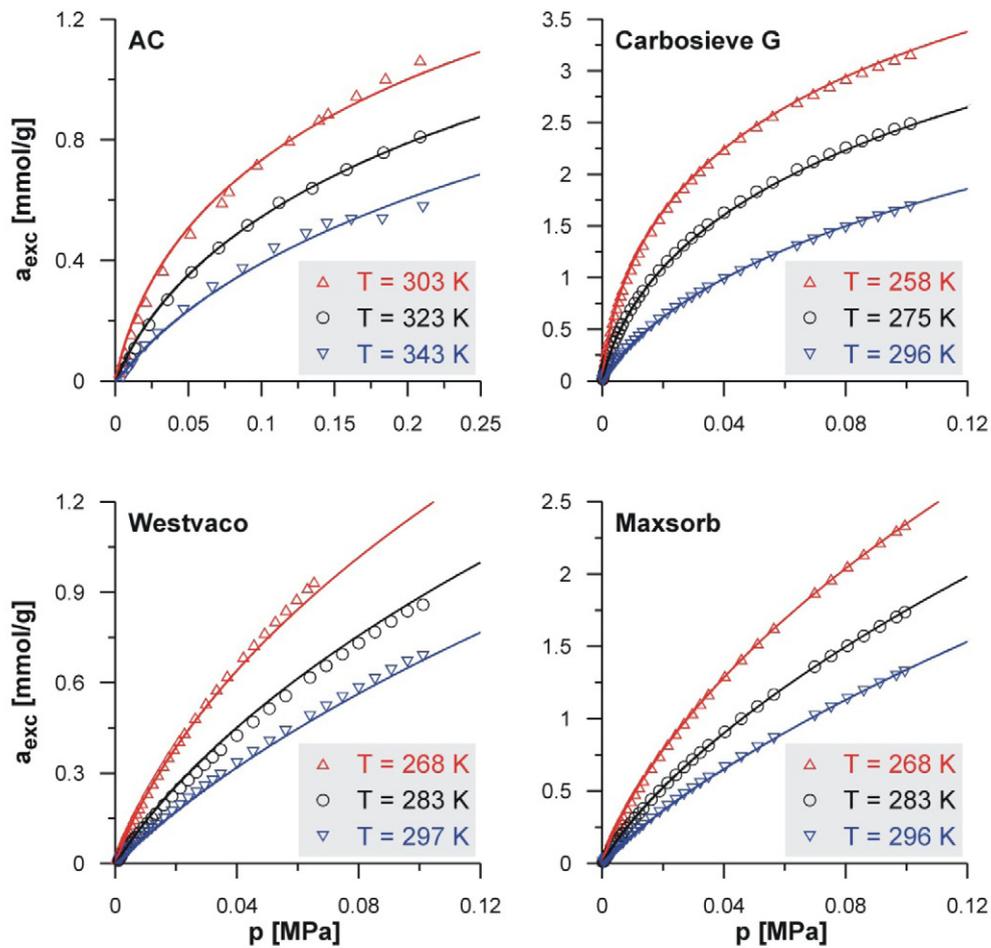
SIMULATION

Figure 4. Graphical representation of the fitting of experimental adsorption and selected simulation isotherms using the DA model (equations (1)–(4)). Points—experimental and/or simulation data, lines—the model.

collected in table 1. One can observe an excellent fit for the experimental as well as the simulated data.

   The regularities observed on simulated adsorption isotherms are reflected by the values of parameters obtained

from the fitting. As one can see from table 1 the decrease in adsorption capacity (limited by the pore volume) from S0 down to the S35 structure leads to the decrease in the value of the a_0^B parameter. The decrease in the pore diameter leads

Table 1. The values of the best-fit parameters obtained using the DA model (equations (1)–(4)) to describe the experimental (a) and simulated (b) data. The average pore diameters are also presented (taken from the literature for real carbon samples and calculated from equation (9) for VPCs).

Carbon	d_{av} (nm)	a_0^B (mmol g^{-1})	E (kJ mol^{-1})	n	k	DC_T[a]	DC
(a) Experimental data							
AC	0.59 [11]	3.09 ± 0.35	10.89 ± 0.56	2.07 ± 0.15	2.75 ± 0.17	0.9935; 0.9977; 0.9886	0.9923
Carbosieve G	0.56 [41]	8.30±0.11	10.863±0.073	2.106±0.022	4.611±0.039	0.9996; 0.9996; 0.9997	0.9996
Westvaco	1.873 [42]	7.1±1.2	7.12±0.12	1.66±0.11	2.70±0.12	0.9967; 0.9951; 0.9968	0.9961
Maxsorb	2.12 [43]	18.34±0.43	6.266±0.086	1.473±0.016	2.960±0.024	0.9998; 1.0000; 0.9998	0.9999
(b) Simulated data							
S0	1.197	16.598 ± 0.022	7.387 ± 0.019	1.3930 ± 0.0046	2.451±0.029	0.9999; 1.0000; 1.0000	1.0000
S4	1.000	15.291 ± 0.025	7.970 ± 0.030	1.5387 ± 0.0075	2.571±0.044	0.9999; 0.9999; 0.9999	0.9999
S8	0.888	13.858 ± 0.022	8.632 ± 0.038	1.666 ± 0.010	2.643±0.055	0.9999; 0.9999; 0.9999	0.9999
S12	0.823	12.434 ± 0.019	9.208 ± 0.041	1.736 ± 0.011	2.699±0.060	0.9999; 0.9999; 0.9999	0.9999
S16	0.782	11.021 ± 0.017	9.679 ± 0.046	1.782 ± 0.012	2.738±0.067	0.9998; 0;9999; 0.9999	0.9999
S20	0.745	10.319 ± 0.016	9.997 ± 0.051	1.819 ± 0.013	2.768±0.074	0.9998; 0.9999; 0.9999	0.9999
S24	0.713	9.594 ± 0.015	10.230±0.051	1.822 ± 0.014	2.799±0.076	0.9998; 0.9999; 0.9999	0.9999
S28	0.689	8.964 ± 0.015	10.478±0.056	1.845 ± 0.013	2.835±0.081	0.9998; 0.9999; 0.9999	0.9999
S32	0.673	8.311 ± 0.013	10.663±0.053	1.833 ± 0.013	2.932±0.077	0.9998; 0.9999; 0.9999	0.9999
S35	0.661	7.844 ± 0.013	10.762±0.057	1.848 ± 0.014	3.001±0.083	0.9998; 0.9999; 0.9999	0.9999

[a] The values arranged according to the rise in temperature.

to a greater characteristic energy of adsorption; at the same time we observe a decrease in the maximum adsorption value. Different types of relationships between E_0 and the pore diameter have been proposed in the literature for adsorbed subcritical and supercritical gases. The simplest of them are inverse relations (see for example [34] and references therein). However, there are no reports showing these types of relations for CF$_4$ adsorption.

As one can observe in figure S1 in the supplementary data (available at stacks.iop.org/JPhysCM/25/015004/mmedia) the data obtained from simulations performed in this study lead to an inverse-type relationship between both values. Moreover, from this relationship, knowing the experimental value of E_0 one can easily estimate the pore diameter from the experimental data.

As one can also see, k and n depend almost linearly on the reverse effective pore diameter of the studied carbon. It is very important that the empirical parameter of Amankwah and Schwarz relation (equation (3)) is strictly related with the average diameter of carbon micropores. It is significant that the experimental data fit well with our simulation results. If we compare simulation with experiment we can see that for the AC carbon having, according to the producers, an average pore diameter of 0.59 nm [11] the values of E and n (10.89 kJ mol^{-1} and 2.07, respectively) are slightly larger than observed for the VPC structure S35 (10.762 kJ mol^{-1} and 1.848, respectively), having the smallest average pore diameter (i.e. 0.661 nm). Similar E and n values as for carbon AC are observed for Carbosieve G (E = 10.863 kJ mol^{-1}, n = 2.106, see table 1), therefore in this case we can expect a similar pore diameter as for the AC carbon i.e. similar and equal to 0.56 nm [41]. In contrast, for the two remaining adsorbents (Westvaco and Maxsorb) the pore diameters submitted in the literature are considerably larger (table 1) and this is the reason for considerably smaller E and n values, since the pore size distribution in this case should be wider.

In figure 5 we collect all the data considered in this study. As can be observed there is quite good agreement between simulation and experiment. The data collected in figure 5 explain the experimental observation, and allow us to predict the adsorption properties towards CF$_4$ for other carbons. The slightly worse relation between n and inverse pore diameter is probably caused by the fact that n, as the heterogeneity measure, should be rather correlated with the width of the pore size distribution. The values of parameter k for the experimental data do not fit the simulation results. This is the reason why we omitted this in the manuscript. It is obvious that a simple, nanometric scale model of carbon is not a model of a real sample studied experimentally. But, as can be concluded from obtained results, it is a good approach for the real structure.

As was widely accepted in literature, so-called DA plots (i.e. the plots of the isotherms in the linear coordinates of the DA equation) can be useful for the discussion of the mechanism of adsorption. Since the parameter n for all studied systems was calculated by us (see table 1) we can easily construct DA plots and they are collected in figures S2 and S3 (supplementary data available at stacks.iop.org/JPhysCM/25/015004/mmedia). Considering the DA plots for selected simulation data (figure S2 available at stacks.iop.org/JPhysCM/25/015004/mmedia) one can see that they are bimodal, i.e. they are composed of two straight lines. The plots become more linear with the rise in temperature and with the rise in the number of small micropores in the system. Thus we can state that the mechanism of primary and secondary micropore filling occurs. In contrast, for experimental data (figure S3 available at stacks.iop.org/JPhysCM/25/015004/mmedia) we apparently observe the linearity of DA plots. In our opinion, this could be caused by the lack of experimental points measured at higher pressures.

As one can easily see, the most promising CF$_4$ adsorbent should possess micropores with a diameter around 0.5 nm, and
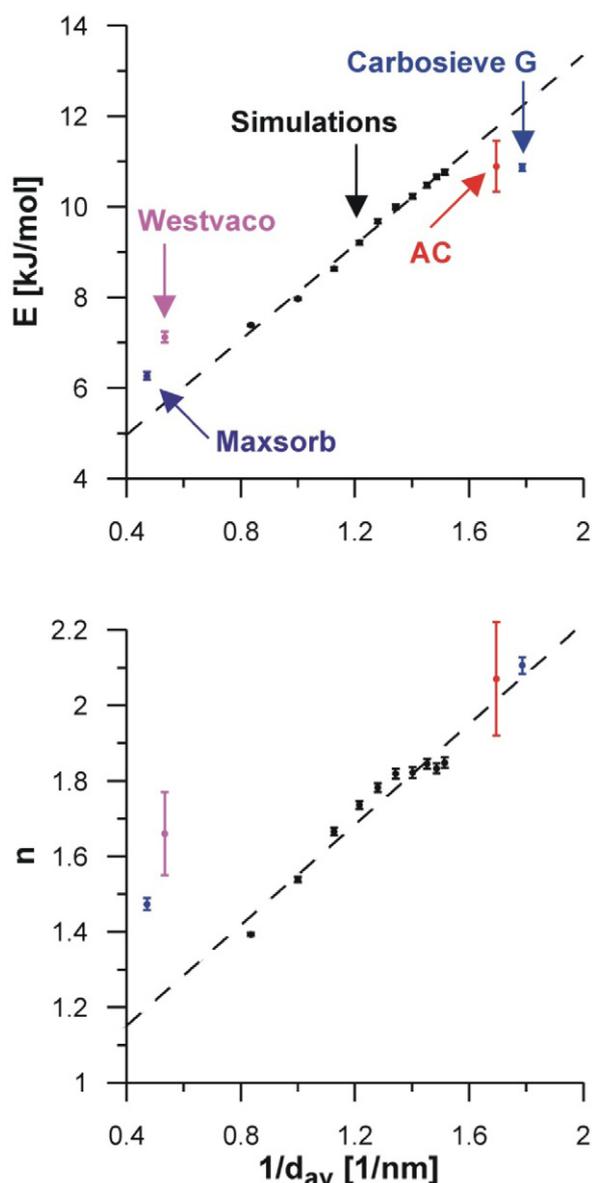
Figure 5. Comparison of characteristic energy and *n* values for experimental and simulated data (table 1) as a function of reciprocals of the average pore diameters (d_{av}).

the diameters should be as homogeneous as possible (i.e. n should be larger than 2). However, more importantly, there are linear relationships between the empirical parameters of the modified DA equation and micropore diameters. Moreover, the same linear relationship occurs between *k* and the average pore diameter. In this way, systematic computer simulation studies help to assign the meaning of the empirical parameters.

4. Conclusions

The results of this study show that molecular simulations are very powerful for the investigation of adsorption of the greenhouse gas CF$_4$ on carbons. We show for the first time, that the application of VPC models leads to results which are in good agreement with experimental data available in the literature. Experimental data fitted general correlations obtained from Monte Carlo simulations. Importantly, we show not only the general relationships, but are able, for the first time, to explain the physical meaning of the parameters of the empirical DA adsorption isotherm equation. Thus, we show that these parameters are related to the average micropore diameter of the studied carbons.

Our results also lead to the conclusion that the supercritical version of the DA model proposed by Ozawa is a very powerful tool and should be successfully applied to the description of experimental data. Since in the current study we related the empirical parameters of the DA model (used with the empirical Amankwah and Schwarz relation to describe the CF$_4$ adsorption data) to the parameters of carbon structure we hope that the results of this study will shed new light on the regularities observed during adsorption of this greenhouse gas.

References

[1] Müller E A 2005 *Environ. Sci. Technol.* **39** 8736
[2] Kowalczyk P and Holyst R 2008 *Environ. Sci. Technol.* **42** 2931
[3] Bottani E J and Tascón J M D (ed) 2008 *Adsorption by Carbons* (Amsterdam: Elsevier)
[4] Bansal R Ch and Goyal M 2005 *Activated Carbon Adsorption* (Boca Raton, FL: Taylor and Francis)
[5] Marsh H and Rodríguez-Reinoso F 2006 *Activated Carbon* (Amsterdam: Elsevier)
[6] Tascón J M D (ed) 2012 *Novel Carbon Adsorbents* (Amsterdam: Elsevier)
[7] Saha B B and Ng K Ch (ed) 2010 *Advances in Adsorption Technology* (New York: Nova Science)
[8] Jagiełło J, Bandosz T J, Putyera K and Schwarz J A 1995 *J. Chem. Eng. Data* **40** 1288
[9] Jagiełło J, Bandosz T J and Schwarz J A 1996 *Langmuir* **12** 2837
[10] Singh S, Tezel F H and Harlick P J E 2002 *Sep. Sci. Technol.* **37** 2763
[11] Ahn N-G, Kang S-W, Min B-H and Suh S-S 2006 *J. Chem. Eng. Data* **51** 451
[12] Biggs M J and Buts A 2006 *Mol. Simul.* **32** 579
[13] Gauden P A, Terzyk A P and Furmaniak S 2008 *Wiadomości Chemiczne* **62** 403
[14] Terzyk A P, Furmaniak S, Gauden P A, Harris P J F, Wesołowski R P and Kowalczyk P 2011 *Activated Carbon: Classification, Properties and Applications* ed J F Kwiatkowski (New York: Nova Science) pp 355–76
[15] Terzyk A P, Furmaniak S, Gauden P A, Harris P J F and Kowalczyk P 2012 *Novel Carbon Adsorbents* ed J M D Tascón (Amsterdam: Elsevier) pp 61–104
[16] Harris P J F and Tsang S C 1997 *Phil. Mag.* A **76** 667

[17] Harris P J F 1997 *Int. Mater. Rev.* **42** 206
[18] Harris P J F, Burian A and Duber S 2000 *Phil. Mag. Lett.* **80** 381
[19] Harris P J F 2005 *Crit. Rev. Solid State Mater. Sci.* **30** 235
[20] Harris P J F, Liu Z and Suenaga K 2008 *J. Phys.: Condens. Matter* **20** 362201
[21] Harris P J F 2008 *Carbon Materials—Theory and Practice* ed A P Terzyk, P A Gauden and P Kowalczyk (Kerala: Research Signpost) pp 1–14
[22] Harris P J F 2013 *J. Mater. Sci.* at press
[23] Stoeckli F 2001 *Russ. Chem. Bull.* **50** 2265
[24] Kadlec J 2001 *Adsorpt. Sci. Technol.* **19** 1
[25] Terzyk A P, Furmaniak S, Gauden P A, Harris P J F and Włoch J 2008 *J. Phys.: Condens. Matter* **20** 385212
[26] Terzyk A P, Furmaniak S, Wesołowski R P, Gauden P A and Harris P J F 2010 *Advances in Adsorption Technology* ed B B Saha and K C Ng (New York: Nova Science) chapter 14
[27] Amankwah K A G and Schwarz J A 1995 *Carbon* **33** 1313
[28] Ozawa S, Kusumi S and Ogino Y 1976 *J. Colloid Interface Sci.* **56** 83
[29] Storn R and Price K 1997 *J. Glob. Optim.* **11** 341
[30] Furmaniak S, Gauden P A, Terzyk A P and Rychlicki G 2008 *Adv. Colloid Interface Sci.* **137** 82
[31] Furmaniak S, Terzyk A P, Gołembiewski R, Gauden P A and Czepirski L 2009 *Food Res. Int.* **42** 1203
[32] Furmaniak S, Terzyk A P and Gauden P A 2011 *Drying Technol.* **29** 984
[33] Furmaniak S 2012 *Transp. Porous Media* **92** 21
[34] Terzyk A P, Furmaniak S, Gauden P A, Harris P J F, Włoch J and Kowalczyk P 2007 *J. Phys.: Condens. Matter* **19** 406208
[35] Bhattacharya S and Gubbins K E 2006 *Langmuir* **22** 7726
[36] Furmaniak S, Terzyk A P, Gauden P A, Harris P J F and Kowalczyk P 2009 *J. Phys.: Condens. Matter* **21** 315005
[37] Furmaniak S, Terzyk A P, Gauden P A, Marks N A, Powles R C and Kowalczyk P 2011 *J. Colloid Interface Sci.* **360** 211
[38] Yan Q and de Pablo J J 1999 *J. Chem. Phys.* **111** 9509
[39] Frenkel D and Smit B 1999 *Understanding Molecular Simulation* (San Diego, CA: Academic)
[40] Steele W A 1974 *The Interaction of Gases with Solid Surfaces* (Oxford: Pergamon)
[41] Hong A, Mariwala R K, Kane M S and Foley H C 1995 *Ind. Eng. Chem. Res.* **34** 992
[42] Karanfil T and Kilduff J E 1999 *Environ. Sci. Technol.* **33** 3217
[43] Takeuchi Y, Hino M, Yoshimura Y, Otowa T, Izuhara H and Nojima T 1999 *Sep. Purif. Technol.* **15** 79